International Journal of Pharmaceutics 404 (2011) 83–93

Contents lists available at ScienceDirect

International Journal of Pharmaceutics

journal homepage: www.elsevier.com/locate/ijpharm

Magnetic microparticles based on natural polymers

G. Tataru[a,b], M. Popa[a], J. Desbrieres[b,*]

[a] Technical University «Gheorghe Asachi», Faculty of Chemical Engineering and Protection of the Environment, Department of Natural and Synthetic Polymers, 73, Bd. Prof. Dr. doc. Dimitrie Mangeron, 700050 IASI, Romania
[b] Pau et Pays de l'Adour University, IPREM/EPCP (UMR CNRS 5254), Helioparc Pau Pyrénées, 2 Avenue P. Angot, 64053 PAU cedex 09, France

ARTICLE INFO

Article history:
Received 22 April 2010
Received in revised form 4 November 2010
Accepted 5 November 2010
Available online 12 November 2010

Keywords:
Magnetic particles
Network
Carboxymethylcellulose
Gelatin
Maghemite
Cefotaxime
Methotrexate
Drug controlled release

ABSTRACT

Magnetic micro- and nanoparticles based on ferrofluid (maghemite) were elaborated by inverse emulsion crosslinking of sodium salt of carboxymethylcellulose (CMCNa) and gelatin. Crosslinking was carried out with glutaric aldehyde within aqueous droplets dispersed into toluene in presence of surfactants. The influence of parameters such as the ratio of polymers and maghemite in the initial mixture on the composition, size, size dispersity, particle swelling and their ability for drug inclusion was studied. The ability to take-up drugs is directly correlated with the degree of swelling and gelatin content within the particles. Particle size is between tens of nanometers and a few microns. The magnetic properties of particles are demonstrated from saturation magnetization (between 43 and 44 emu g^{-1}) when their superparamagnetic character was shown by the absence of hysteresis on the magnetization curve. Polymer–drug systems elaborated under particles keep their bactericide activity for at least 48 h. The absence of toxicity, associated with the bactericide activity, make these systems potential drug carriers.

1. Introduction

Magnetic microparticles are being called upon for possible applications in biomedics due to their physico-chemical properties. They have controllable dimensions, within the range of a few nanometers to 10 μm, making them of a size comparable to cells (10–100 μm), viruses (20–450 nm), proteins (5–50 nm) and genes (2 μm width and 10–100 nm length). This indicates that they may have close but controlled contact with biological targets (McBain et al., 2008; Laurent et al., 2008; Ma and Liu, 2007). They are subject to Coulomb's law, and respond to magnetic fields by moving in the direction of field lines. This "control at a distance" combined with the intrinsic penetrability of magnetic field through the human body, open new horizons for many applications including the immobilization and/or the transport of biologically active matter, along with the targeting of biological entities. So, magnetic microparticles may be used as vectors, and/or substance carriers for example of antitumor drugs and radioactive atoms towards a specific target of an organism, such as a tumor tissue (Pankhurst et al., 2003; Ruiz-Hernandez et al., 2008). Magnetic microparticles respond by resonance with an alternating magnetic field, allowing the transfer of energy from the energy field towards the microparticle. As a consequence, particles may heat up, leading to the idea of their use in hyperthermy, or the release of controlled quantity of toxic drug by thermal effects within a target tissue, such as the aforementioned tumor tissue as a moderate temperature increase in tissues leads to a more efficient destruction of cancerous cells (Levy et al., 2008; Goya et al., 2008).

The most widely known and used magnetic particles are ferrofluids due to advantages they have compared to other particles: they are compatible with living organisms, they present an excellent *in vivo* stability, and they migrate easily under magnetic fields. After much research, Lübbe et al. (1996a,b) obtained, in 1996, particles with diameters around 100 nm on to which epirubucin was chemically bound. These nanoparticles were clinically tested with promising results.

A more widely studied technique over the last few years has been the coating of magnetic particles with biodegradable and biocompatible polymers (natural or synthetic), offering the supplementary possibility to more efficiently include or chemically bind various active matter, insuring simultaneously their transport towards the target (often a tumor). Such systems, formed by a polymer matrix (as particles) containing magnetic nanoparticles and drugs are grown on under the terms of "drug delivery polymeric magnetic particles". Such a system was elaborated by Widder et al. (1979). These are microparticles based on albumin (diameter *ca* 0.2–2 μm) containing Fe_3O_4 as magnetic nanoparticles (diameter of 10–20 nm) and doxorubicin as a therapeutic agent. Such a system may be administered by a parental route (intravenous or intra-arterial). Then an external magnetic field was applied to guide

* Corresponding author. Tel.: +33 (0)5 59 40 76 02; fax: +33 (0)5 59 40 76 23.
E-mail address: jacques.desbrieres@univ-pau.fr (J. Desbrieres).

0378-5173/$ – see front matter © 2010 Elsevier B.V. All rights reserved.
doi:10.1016/j.ijpharm.2010.11.002

and concentrate this complex towards the infected zone (usually a tumor).

Many systems of this kind were developed during last years using various elaboration processes. Matrixes used were either natural or artificial (modified natural) polymers such as chitosan (Hassan et al., 1992), albumin (Widder et al., 1979; Bellusci et al., 2009), hydroxypropylcellulose (Nagano et al., 1997), starch, pectin, alginates (Bergemann et al., 1999; Alexiou et al., 2001) or synthetic poly(vinyl alcohol) (Bergemann et al., 1999), poly(lactic acid) (Ramanujan and Chong, 2004), poly(2-ethylcyanoacrylate) (Arias et al., 2005), poly(vinylpyrrolidone) (Chen et al., 2005), poly(ethylene glycol) (Kohler et al., 2006) or poly(ε-caprolactone) (Yang et al., 2006).

The objective of this work is the elaboration, by inverse emulsion crosslinking, of magnetic micro- and nanoparticles based on ferrofluid (maghemite) included within an interpenetrating polymer network hydrogel matrix of carboxymethylcellulose (CMCNa) and gelatin, and their characterization. To the best of our knowledge such particles have not been described in the literature. They present the advantage of an easy elaboration process combined to low cost, biocompatible and non-toxic natural polymers.

2. Materials and methods

2.1. Materials

Carboxymethylcellulose under sodium salt (CMCNa) was purchased by Fluka. Its degree of substitution was 0.75 as determined by gravimetric methods and confirmed by atomic absorption spectrometry, and its weight-average molar mass was 300,000 g mol^{-1}. Type A Gelatin (GEL) from Sigma Aldrich was characterized as having a molecular weight of 100,000 g mol^{-1}, an isoelectric point equal to 6.73, an average NH_2 content of 0.954 mmol g^{-1}. Glutaric aldehyde (AG) from Sigma Aldrich, the crosslinking agent, was used as 25% aqueous solution. Tween 80 from Aldrich was a non-ionic surfactant used for stabilizing the emulsions. Its hydrophile–lipophile balance (HLB) was 15.0. Its composition was predominantly oleic acid, and linoleic, palmitic and stearic acids. Span 80, supplied by Aldrich, has an HLB value of 4.3. It is often used in pharmaceutical industry as a surfactant to stabilize emulsions. Brij 52 is a non-ionic surfactant (ethoxylated alcohol) from Croda with an HLB value of 5.3.

The nanofluid based on maghemite (Fe_3O_4) was obtained in the laboratory using Massard method (Massart, 1980). The quoted dry residue (solid concentration) is equal to 9% and the average particle diameter is 20 nm (from laser diffraction analyzer). Cefotaxime (CFTS) is a water soluble (sodium salt) antibiotics used for the treatment of severe infections by germs located in the respiratory tract, genito-urinary system or to treat intra-abdominal infections. Methotrexate (MTX) is a drug used for cancer treatment (mammary cancer, non-Hodgkin lynphom, etc.). It is supplied by Fluka as a solution in NaOH 0.1 mol L^{-1}.

2.2. Preparation of magnetic particles

Elaboration of magnetic polymeric particles was carried out using an inverse emulsion process. The aqueous phase, in which are the polymers to be crosslinked and the nanofluid, was dispersed in a nonmiscible organic phase (toluene). To stabilize this emulsion which had an HLB value of 6.5 a mixture of two surfactants was used: a hydrophobic (Brij 52, HLB = 5.3, respectively, Span 80, HLB = 4.3) and a hydrophilic one (Tween 80, HLB = 15). Brij was chosen because it is one of the few surfactants to act in a strongly acid medium due to the nanofluid (pH = 3). The concentration of the surfactant mixture was determined according to the experimental design presented in Table 1 and calculated from the relation (1)

Table 1
Experimental design for obtaining magnetic particles based on CMCNa and GEL crosslinked with AG.

Particles series	Samples series	Initial content of components[c]			Polymers/AG ratio[d] (r_{PA}, g/g)	Polymers/maghemite ratio (r_{PM}, g/g)	Concentration of surfactant (C_t, %)	Sizes of nanoparticles (μm)
		CMCNa (%)	GEL (%)	γ-Fe_2O_3 (%)				
	MMGB1	0	64					0.91 ± 0.01
	MMGB2	12.8	51.2					0.88 ± 0.01
	MMGB3	25.6	38.4					0.86 ± 0.01
1[a]	MMGB4	32	32	36	71.43	1.77	0.225	0.37 ± 0.01
	MMGB5	38.4	25.6					0.38 ± 0.01
	MMGB6	41.2	12.8					0.31 ± 0.02
	MMGB7	64	0					0.30 ± 0.01
	MMGB17				47.62			0.07 ± 0.01
	MMGB16				57.14			0.30 ± 0.01
2[a]	MMGB5	38.4	25.6	36	71.43	1.77	0.225	0.38 ± 0.01
	MMGB15				119.05			0.39 ± 0.01
	MMGB8	28.2	18.8	53.0		0.88		0.07 ± 0.01
	MMGB9	33.6	22.4	44.0		1.27		0.14 ± 0.01
3[a]	MMGB5	38.4	25.6	36	71.43	1.77	0.225	0.38 ± 0.02
	MMGB10	44.9	29.9	25.2		2.96		0.86 ± 0.03
	MMGB11	48.9	32.7	18.4		4.44		0.88 ± 0.09
	MMGB12						0.1	0.86 ± 0.04
4[a]	MMGB5	38.4	25.6	36	71.43	1.77	0.225	0.38 ± 0.02
	MMGB13						0.5	0.39 ± 0.03
	MMGB14						1	0.39 ± 0.01
	MMGS1						0.5	4.80 ± 0.03
	MMGS2						1.0	4.79 ± 0.03
	MMGS3						1.5	4.57 ± 0.02
1[b]	MMGS6	38.4	25.6	36	71.43	1.77	2	4.61 ± 0.03
	MMGS5						3	4.47 ± 0.02
	MMGS4						4	4.33 ± 0.02

[a] The mixture of surfactants is formed by Brij 52 and Tween 80.
[b] The mixture of surfactants is formed by Span 80 and Tween 80.
[c] The percentage of CMCNa, GEL and γ-Fe_2O_3 was calculated relative to the total quantity of components (mass).
[d] AG is extracted into toluene (50:50, v/v), 1 ml toluene saturated in AG contains 1.12 mg AG.

(Verdinelli et al., 2008):

$$\%\,\text{Hydrophilic surfactant} = \frac{\text{HLB}_{\text{emulsion}} - \text{HLB}_{\text{hydrophobic surfactant}}}{\text{HLB}_{\text{hydrophilic surfactant}} - \text{HLB}_{\text{hydrophobic surfactant}}} \times 100 \quad (1)$$

In a three-necked reactor, the hydrophilic surfactant solution in toluene was prepared under mechanical stirring (800 rpm). Then the aqueous maghemite nanofluid was introduced within the organic phase (142 mL) as very fine droplets. After 10 min, the polymeric aqueous solution containing the hydrophilic surfactant (which pH is adjusted to 3 with glacial acetic acid) was dropped. When the dispersion was homogeneous (after around 30 min), the crosslinking agent (8 mL of toluene saturated with glutaric aldehyde (Longo et al., 1982)) was introduced, this instant being origin time of the reaction. At the end of the reaction the emulsion was "broken" by centrifugation (10 min, 6000 rpm). The organic phase was eliminated and particles were washed by successive washing-separation cycles on a magnetic plate. The washing step was carried out alternately with water and acetone, to eliminate products which have not reacted, secondary products and toluene traces. After a final washing in acetone, particles were dried first in an oven at 40 °C and then under vacuum (24 h, 20 °C).

2.3. Analysis techniques

2.3.1. FTIR spectroscopy

FTIR spectra were recorded with Digilab Scimitar FTS 200 (USA) with KBr pellets.

2.3.2. Scanning Electron Microscopy

Electroscan E3 (20 kV) microscope was used and surface plating was not necessary.

Size analysis and polydispersity of particles were carried out using a Shimadzu SALD 7001 laser diffraction analyzer (purple, $\lambda = 405$ nm). Particles were suspended in acetone to avoid their swelling and obtain a value of the equivalent diameter close to dry state. The apparatus had a stirring system to keep the particles in suspension. For each measure, five samples were considered. Surface diameter (sphere of the same surface area) was determined.

2.3.3. Composition

According to the studied compound the technique was adapted.

The gelatin content was measured by the Nitrogen content using Kjeldahl method (Bradstreet, 1965).

To determine the γ-Fe_3O_4 content, two methods were used:

- Thermogravimetric measurement using a TA Instruments 2950 thermobalance between 30 and 900 °C, at a temperature rate of 10 °C min^{-1} under nitrogen atmosphere. It was determined from the relation (2):

$$M_{\gamma\text{-}Fe_2O_3} = R_{\text{pmg}} - \frac{R_{\text{p}} \times (M_{\text{f,pmg}} - M_{\text{i,pmg}})}{M_{\text{f,p}} - M_{\text{i,p}}} \quad (2)$$

  where $(M_{\text{f,p}} - M_{\text{i,p}})$ and $(M_{\text{f,pmg}} - M_{\text{i,pmg}})$ are the weight loss for polymeric and magnetic particles respectively (in %), R_{p} and R_{pmg} the residues at 900 °C of polymeric and magnetic particles respectively (in %), and $M_{\gamma\text{-}Fe_2O_3}$ the maghemite content of magnetic particles (in %).
- Atomic absorption spectroscopy using an air–acetylene flame, the specific wavelength for iron being 248.3 nm. A calibration curve was beforehand built and the maghemite content was determined from relation (3):

$$\gamma\text{-}Fe_2O_3 = \frac{C_{\text{Fe,IPN}}/10}{a \times 0.7 \times 1000} \times 100 \quad (3)$$

where a is the weight of the analyzed dry sample (in g), C_{Fe} is the Fe concentration in the analyzed sample (in mg L^{-1}), and 0.7 the Fe content in 1 g of γ-Fe_2O_3 (in g).

2.4. Swelling ratio

Thermogravimetric experiments, using a TA Instruments 2950 thermobalance, permit determination of the swelling ratios of the particles. The characterizations, performed under air, consisted of a ramp from 30 to 120 °C at 10 °C min^{-1} and then temperature was kept constant at 120 °C for 60 min. Samples were immersed in water for predefined durations; excess water was then removed by swabbing with filter paper. The swelling ratio was measured from relation (4):

$$Q_t = \frac{M_t - M_{\text{f}}}{M_{\text{f}}} \times 100 = \frac{m_{H_2O,t}}{m_0} \times 100 \quad (4)$$

where Q_t is the swelling ratio at time t (wt%), M_{f} is the weight of dry sample (in g), M_t is the weight of the swollen sample at time t (in g), $m_{H_2O,t}$ is the weight of adsorbed water at time t (in g) and m_0 the weight of dry sample.

2.5. Inclusion and release of drugs in/from microparticles. UV–visible spectroscopy

Drug inclusion and release were carried out by diffusion of its aqueous solution into/from the particles. Considering inclusion process, 0.05 g of particles at equilibrium swelling are suspended in 50 mL of the drug aqueous solution at known concentration. At determined time intervals, 0.5 mL are removed, diluted to 10 mL with water and analyzed using a UV spectrometer (UV CADAS 1000, Germany) at maximal absorbance wavelength of analyzed drug. These are 236 nm and 302 nm for Cefotaxime and Methotrexate respectively. Calculations are done from calibration curves previously performed.

For drug release kinetics studies, previously loaded particles are centrifuged at 6000 rpm and sediment transferred in a 50 mL volume of twice-distilled water. At determined time intervals, 0.5 mL of solution are removed, diluted to 10 mL and analyzed with the UV spectrometer using the same wavelengths.

2.6. Toxicity of particles

Toxicity is evaluated by the average lethal dose (LD_{50}), which represents the quantity which provokes the death of half of tested animals, in specific experimental conditions. LD_{50} is expressed as mg of active matter per kilogram of adult animal body. Particles are administered *via* the intraperitoneal way, as a suspension in Tween 80, as defined by the Speerman–Karber method (Finney, 1978). Tests were carried out on rats weighing 20 ± 2 g according to the classical laboratory methodology (Czajkowska et al., 1978).

3. Results and discussion

Many hydroxyl or amino groups being along the macromolecular chains of sodium salt of carboxymethylcellulose (CMCNa) and gelatin (GEL) are able to react with glutaric aldehyde (AG). As a consequence, the structure of the material elaborated by crosslinking will be complex and can be considered an interpenetrating polymer network (IPN). Possible crosslinking reactions may be schematized as shown in Scheme 1.

Amino groups from the protein react with AG forming imine-type bonds. Hydroxyl groups from the polysaccharide may form either semi-acetal or acetals. The position of these groups, alternating on both sides of the glucosidic ring, leads to the fact that acetal cycle is the less likely due to the larger distance between hydroxyl

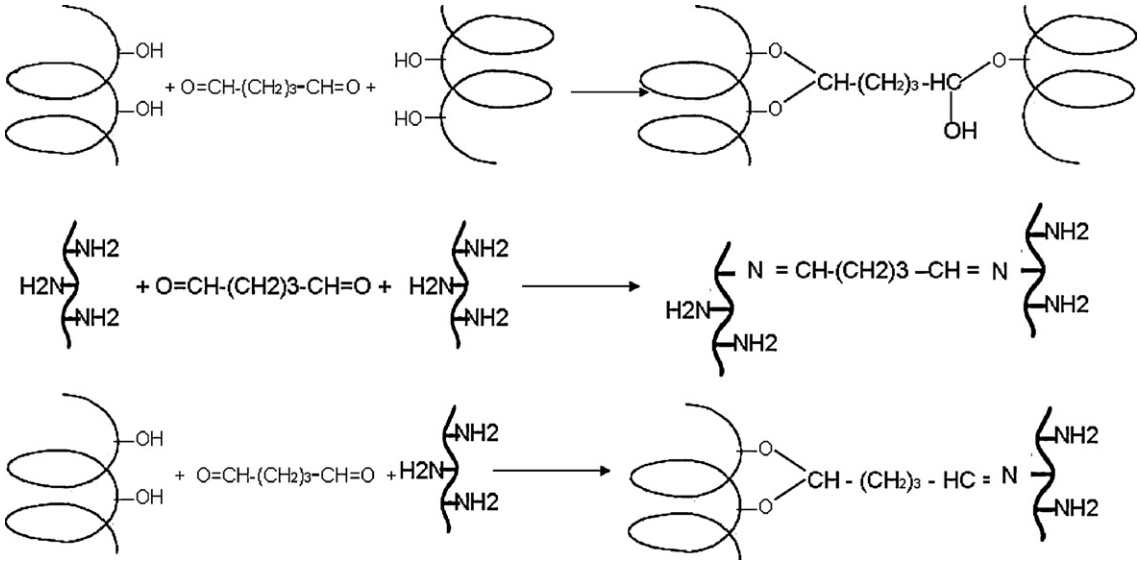

Scheme 1. Crosslinking reactions of CMCNa and GEL with glutaric aldehyde.

groups with which AG has to react. Semi-acetal formation is the most likely. Moreover, semi-acetals are less stable compared to acetals (Nenitescu, 1980) and finally semi-acetal bonds hydrolyze more easily. But if we keep in mind the goal of the preparation of such materials, the formation of semi-acetal bonds may be an advantage because the hydrolysis and biodegradation of particles within human body typical physiological medium will be made easier.

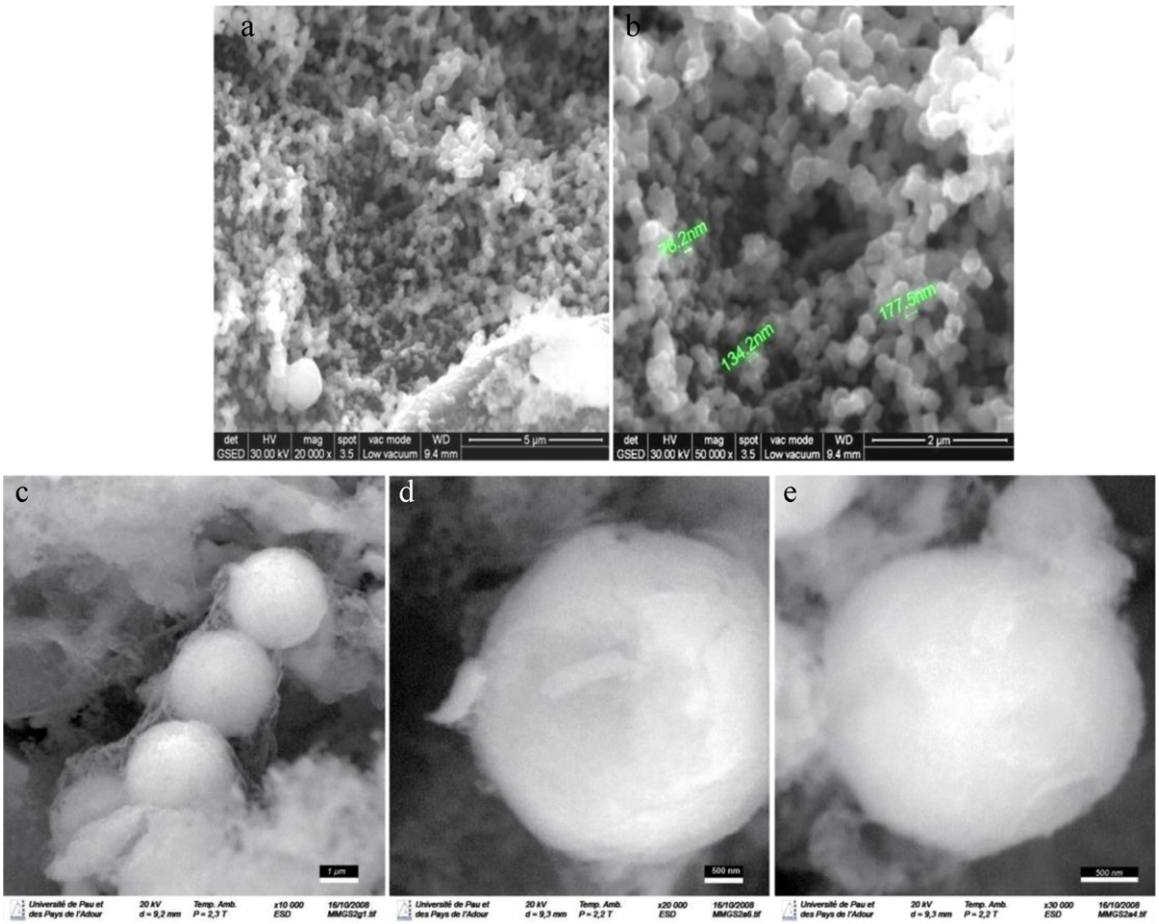

Fig. 1. Scanning Electron Microscopy of MMGB13 particles (a – 10,000×, b – 20,000×) (CMCNa:GEL:γ-Fe_2O_3 = 38:26:36; r_{PA} = 71.43; r_{PM} = 1.77; C_t = 0.5%; surfactants: Brij 52 and Tween 80) and particles MMGS1 (c – 10,000×, d – 20,000×, e – 30,000×) (CMCNa:GEL:γ-Fe_2O_3 = 38:26:36; r_{PA} = 71.43; r_{PM} = 1.77; C_t = 0.5%; surfactants Span 80 and Tween 80).

3.1. Physico-chemical and morphological characterization of particles

FTIR spectra (not shown) demonstrate the crosslinking reaction between CMCNa and GEL macromolecular chains through glutaric aldehyde. All peaks coming from the polymers are observed, moreover a new peak at 1732 cm^{-1} is attributed to –C=N group (see Scheme 1), demonstrating the crosslinking reaction. Peaks within the 630–585 cm^{-1} range show the presence of maghemite iron oxides (Lu et al., 2007; Honga et al., 2007).

Scanning Electron Microscopy (SEM) photographs (Fig. 1) give information on the particles morphology and size. They are of well-defined spherical shape and their surface is smooth. Those obtained in presence of Brij 52 (Fig. 1a and b) have a smaller diameter compared to those obtained with a Tween and Span mixture (Fig. 1c–e).

Magnetic properties of particles are underlined by magnetometric curves registered at 300 K (Fig. 2). Saturation magnetization of MMGB particles reached values between 43.1 and 44.1 emu g^{-1}, respectively, and 44 emu g^{-1} for MMGS particles (Fig. 2a and c). The superparamagnetic character of these particles is demonstrated by the absence of hysteresis ($M_r = 0$ and $H_c = 0$); the magnetization curve passes through the origin of coordinate system (Fig. 2b and d).

To elaborate magnetic particles by inverse emulsion crosslinking, some parameters known to affect particles properties such as their composition, size and swelling ability in water or drug inclusion and release have to be considered. These are on one hand CMCNa/GEL, polymers/crosslinking agent, polymers/maghemite ratios, and on the other the concentration and the nature of the surfactant. To understand the role and the influence of each of these parameters, it is necessary to present some of the process peculiarities. The nanofluid is ionically stabilized by peptisation with 2 M nitric acid, implying a pH around 3. As a consequence, maghemite nanoparticles are enclosed by a cationic protective layer. GEL, an amphoteric polymer, acts as a polycation in this pH range, character determined by protonated amino groups ($pH < pH_{iso}$). CMCNa, in the same conditions, is under an acidic form and it adopts a coil conformation. This favors the intramolecular crosslinking by a lactonization reaction between carboxylic acid and hydroxyl groups of the macromolecular chain.

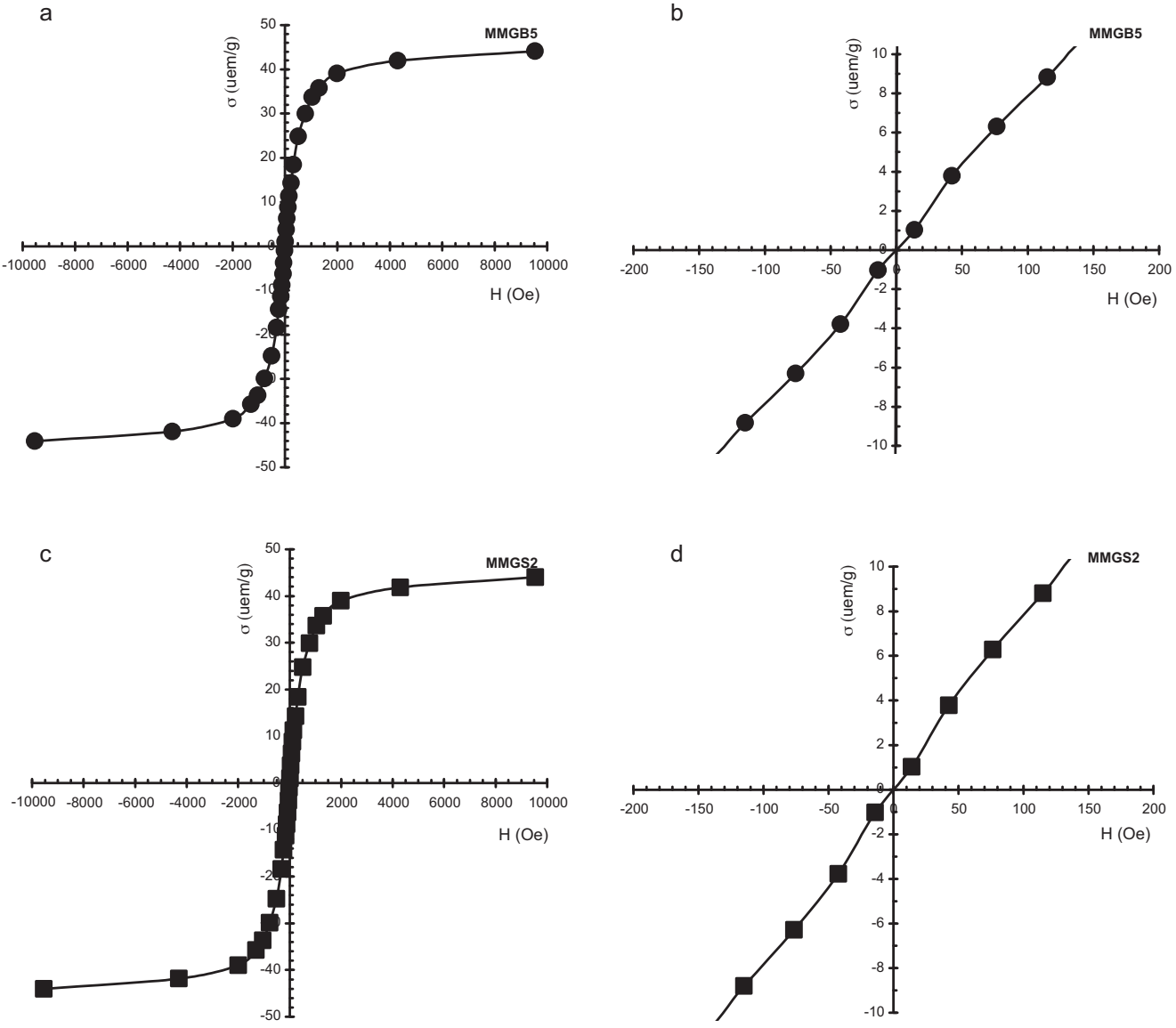

Fig. 2. Magnetization curves of magnetic polymeric particles MMGB5 (a and b) (CMCNa:GEL:γ-Fe_2O_3 = 38:26:36; r_{PA} = 71.43; r_{PM} = 1.77; C_t = 0.225%; surfactants: Brij 52 and Tween 80); and MMGS2 (c and d) (CMCNa:GEL:γ-Fe_2O_3 = 38:26:36; r_{PA} = 71.43; r_{PM} = 1.77; C_t = 1%; surfactants: Span 80 and Tween 80).

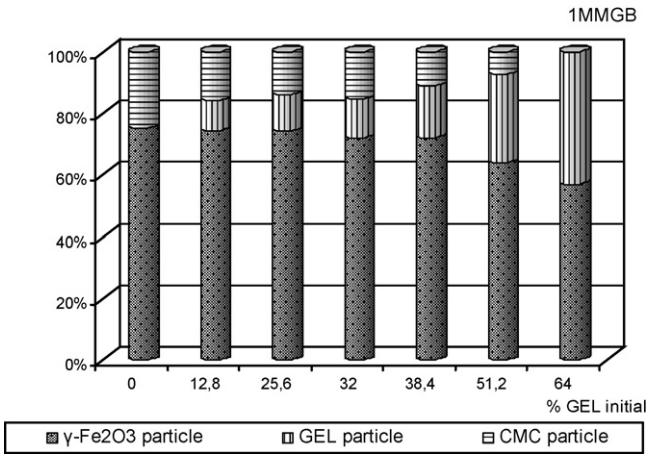

Fig. 3. Influence of the polymer ratio (expressed as GEL concentration) on the composition of MMGB series 1 magnetic particles (polymer/γ-Fe_2O_3 = 64:36; r_{PA} = 71.43; C_t = 0.225%; surfactants: Brij 52 and Tween 80).

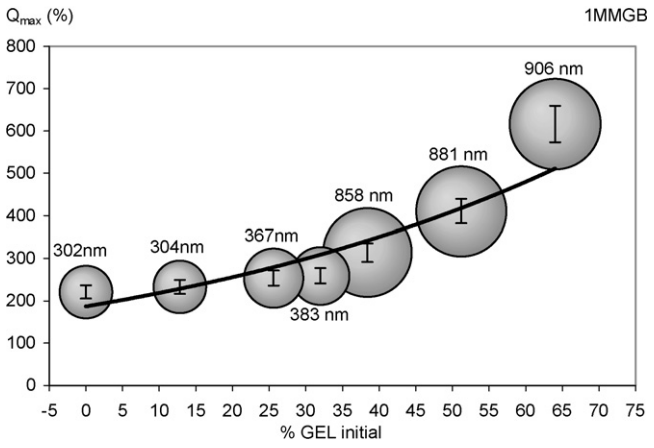

Fig. 5. Influence of the MMGB series 1 magnetic polymeric particles composition and size on the maximal swelling degree (polymers/γ-Fe_2O_3 = 64:36; r_{PA} = 71.43; C_t = 0.5%; surfactants: Brij 52 and Tween 80).

3.2. Role of specific parameters on the particle composition and physico-chemical properties of particles

3.2.1. Influence of CMCNa–GEL ratio

The variation of the composition of the particles as a function of the initial CMCNa/GEL ratio is given in Fig. 3 (it is considered that the polymer mixture represents 64% of the initial material, the supplement being maghemite).

Obviously GEL content in the particles is increasing as a function of its content in the initial mixture. For an initial GEL content of 25%, GEL content in the particles is already larger than CMCNa one. This demonstrates that GEL is more reactive towards AG than CMCNa. It is well interpreted considering the higher nucleophilic effect of amino groups with respect to hydroxyl groups (Nenitescu, 1980).

It was also observed that the highest amounts of included maghemite are obtained in low GEL amount particles. It is easily explained by the fact that the cationic character of protein within the synthetic conditions (acidic pH medium) induces repulsion forces with positively charged nanofluid particles, penalizing their inclusion. Consequently, the maghemite content is decreasing with increasing GEL content within the particles.

Particles do not show a high dispersity and curves are monomodal (Fig. 4).

Average diameter depends on the composition of particles, and increases with GEL content in the initial mixture. It varies between 300 nm (for CMCNa based particles) and 900 nm (for GEL based ones).

The presence of ammonium cations as substituents on the protein chain leads to their extended conformation, favoring the obtaining of a looser crosslinked structure. As a consequence the hydrogel will be less dense, explaining larger particle dimensions due to the increase of GEL content (Fig. 5). Moreover, increasing the GEL content within the initial mixture leads to an increase in the viscosity of the polymer aqueous solution. Considering the same stirring rate, the aqueous solution droplets in which the crosslinking reaction was carried out will be larger. These two correlated factors may explain obtaining of larger particles when protein content was increased.

The maximal swelling ratio in water for this series is increasing with GEL content (from 200% to 600%) and obviously with their size (Fig. 5). This evolution was expected due to the higher hydrophily of protein compared with the polysaccharide and the previously discussed arguments.

3.2.2. Influence of polymer mixture/crosslinking agent ratio

Taking into account the conformation of protein chains in the reaction conditions, the increase of the crosslinking agent content

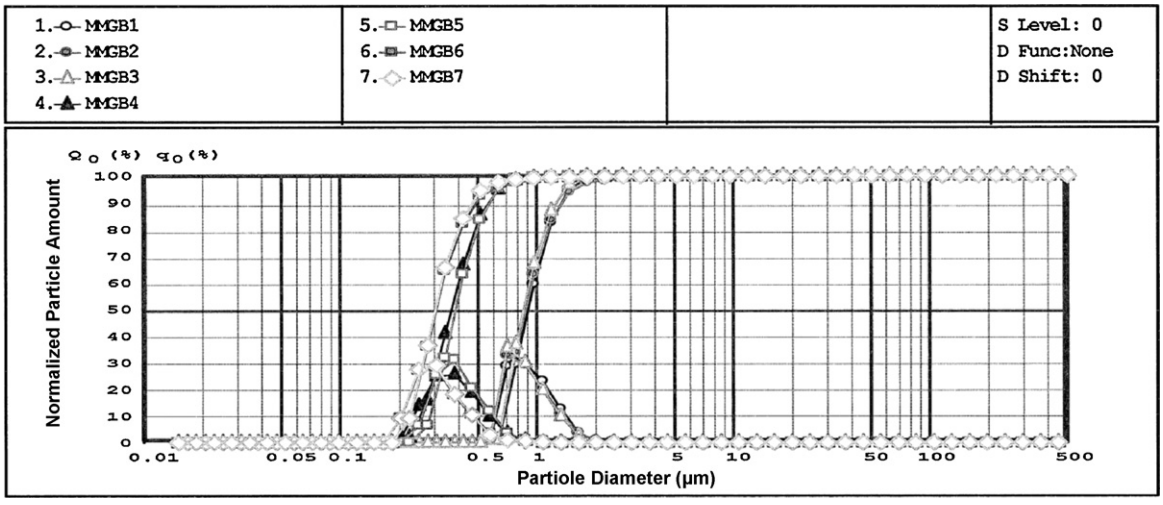

Fig. 4. Size distribution of MMGB series 1 magnetic particles (polymers/γ-Fe_2O_3 = 64:36; r_{PA} = 71.43; C_t = 0.225%; surfactants: Brij 52 and Tween 80).

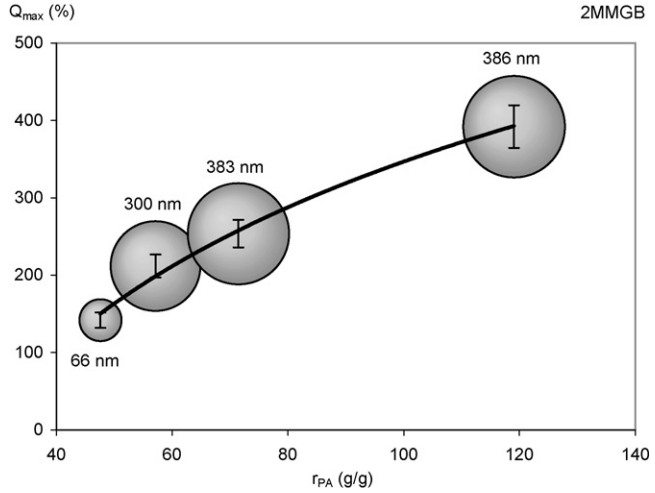

Fig. 6. Influence of the polymers/crosslinking agent ratio (r_{PA}) on the MMGB series 2 particles composition (CMC:GEL:γ-Fe_2O_3 = 38.4:25.6:36; r_{PM} = 1.77; C_t = 0.225%; surfactants: Brij 52 and Tween 80).

shows two effects. First, the most accessible chain conformation will favor bonding of more and more proteins and hence less and less maghemite. Second, the crosslinking density will increase, determining the decrease of the particle size and swelling. GEL content is increasing slightly (from 11% to 16.5%) with decreasing r_{PA} when CMCNa content stays roughly constant around 13%. In the same time the quantity in included maghemite is also decreasing from 75% down to 65%.

The particle diameter is increasing with r_{PA} and it varies within the 66–386 nm range. The evolution of the swelling ratio was explained from the same arguments (Fig. 6).

The size distribution is still monomodal but wider as the particle diameter increased, the latter being between 40 and 750 nm.

3.2.3. Influence of polymers mixture/maghemite ratio

The particle composition, as their morphological characteristics, depends upon the ratio between the amount of polymers and maghemite within the initial mixture. Electrostatic repulsions between magnetic particles stabilized by peptisation and ammonium cations on the GEL chain lead to a decrease of GEL content in the particles (from 25% down to 8.5%) when increasing the nanofluid content in the initial mixture (Fig. 7). Moreover the yield in obtaining particles in this series, defined as the weight ratio between dry magnetic particles and the quantity of components in

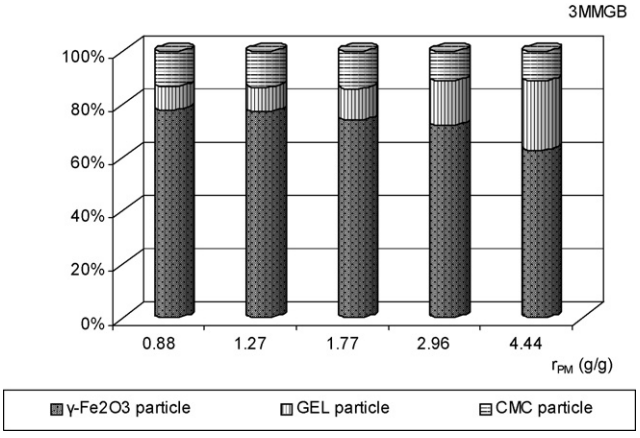

Fig. 7. Influence of polymers/maghemite ratio (r_{PM}) on the MMGB series 3 particles composition (r_{PA} = 71.43; C_t = 0.225%; surfactants Brij 52 and Tween 80).

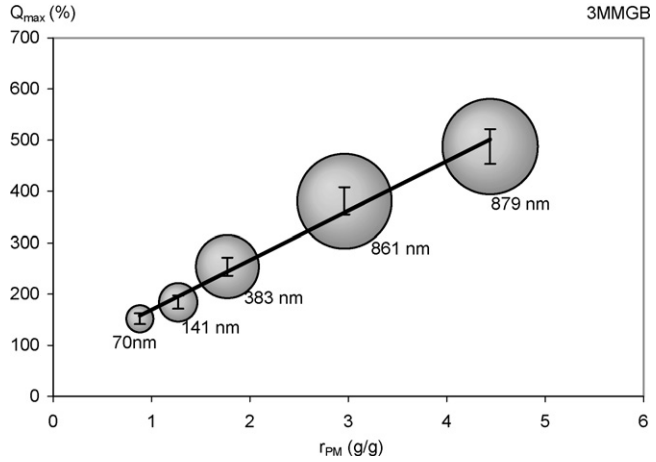

Fig. 8. Influence of polymers/maghemite ratio (r_{PM}) on the MMGB series 3 particles size and swelling degree (r_{PA} = 71.43; C_t = 0.225%; surfactants Brij 52 and Tween 80).

the initial reaction medium, is increasing with polymer/maghemite ratio. Thus it is equal to 42.5% when r_{PM} is 0.88 and increases up to 70.7% when r_{PM} = 4.44.

At the end of the preparation process, some of the magnetic particles may not contain ferrofluid. As the magnetic particles separation at the end of the reaction (and after the successive washing steps with water and acetone) was carried out on a magnetic stirrer, making it quicker; non-magnetic particles are removed, inevitably, with supernatant. This would explain the lower yields obtained when higher polymers/maghemite ratios are used within the initial mixture.

For all magnetic polymeric particles, the major component was maghemite. Their final size increased with r_{PM} in relation with the increase in polymer content and decrease in maghemite one (Fig. 8).

Maximal swelling ratio for this series increased with the polymer/maghemite ratio (Fig. 8) due to the increase in the polymer content, and specially GEL ratio in the polymer mixture. Indeed swelling was increased with hydrophilicity and GEL is the component with the highest hydrophilic nature.

3.2.4. Influence of the surfactant concentration

The role of the surfactant is to initially stabilize the w/o emulsion. The ideal amount of surfactant depends on its critical micellar concentration. The analysis of particles composition as a function of the surfactant concentration leads to observe that at a total surfactant concentration (C_t) smaller than 0.5% (referenced to the emulsion) the composition does not differ significantly even if a small increase in GEL was observed (the final weight composition of the particles is CMCNa:GEL:γ-Fe_2O_3 equal to around 14:12:74). For higher surfactant concentrations (C_t = 1%) GEL content in particles is increasing up to 30% and maghemite one decreasing down to 50% as previously discussed.

From Scanning Electron Microscopy photographs (Fig. 1), the existence of hydrogel parts among particles was observed when synthesis was performed in presence of 0.5% of surfactant. This implies that the quantity of surfactant was not enough to efficiently stabilize the aqueous phase droplets within the organic phase. For a concentration of 1% a better stabilization of the emulsion was realized, and that may explain the larger yield in microparticles observed (78.5% compared to 48.7% when the surfactant concentration was 0.5%). The higher GEL content in the particles is surprising considering that up to a 0.5% surfactant concentration the particle composition was roughly constant. This is due to the fact that increasing the surfactant concentration stabilizes particles and practically no hydrogel was observed among particles (MEB

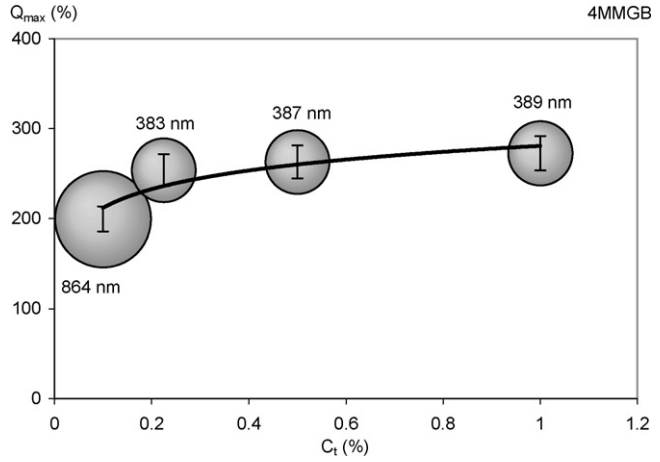

Fig. 9. Influence of the surfactant concentration (Brij 52 and Tween 80) on the MMGB series 4 particles size and maximal swelling degree (CMCNa:GEL:γ-Fe_2O_3 = 38.4:25.6:36; r_{PA} = 71.43).

images not shown). As GEL was the major component of hydrogel, all GEL was contained within particles increasing its relative content compared with CMCNa. The size of particles decreased up to a surfactant concentration equal to 0.23%, and then stays constant. However it was anticipated a continuous decrease of the particle size. It was concluded that, from a threshold surfactant concentration the intensity of the hydrodynamic regime becomes responsible of the particle size. This effect was observed when CMCNa and GEL based particles crosslinked with epichlorohydrine were elaborated (Tataru, 2009). In all experiments the stirring rate was kept constant but according to the surfactant concentration the viscosity will not be the same and hence the hydrodynamic regime may differ.

The maximal swelling ratio of particles increased slightly with polymer content, especially with GEL. The fact that maghemite is the majority component of these particles decreases drastically their ability to swell in water (Fig. 9).

3.2.5. Influence of surfactant nature

To study the influence of the nature of the surfactant, experiments were carried out using a Span 80–Tween 80 mixture. Brij 52 (a hydrophobic surfactant) was replaced by Span 80 and the ratio between the two surfactants was determined so that the HLB (6.5) remained constant. The concentration range was extended between 0.5% and 4.5% (expressed as g surfactant per mL emulsion).

The composition of particles shows very different data compared with previous experiments obtained with other surfactants (Fig. 10). The maghemite content was reduced by 50% but slightly increased with the surfactant concentration. Simultaneously, the GEL content decreased slightly, as expected. It is obvious that this surfactant mixture does not favor the inclusion of the nanofluid, strongly acidic, within the polymer matrix due to the absence of Brij surfactant, known to be one of the only one to act in a strongly acid medium.

The size of the particles is clearly larger than that obtained with Brij surfactant. This demonstrates that it is more suitable to stabilize acid emulsions. Even if the average diameter of the particles does not change greatly with surfactant concentration, a small decrease was observed, as expected.

As the maghemite content is decreasing and the GEL content is increasing compared with the previous surfactant mixture, the swelling ratio was larger (Fig. 11). The reduction of GEL content with increasing of surfactant concentration affects noticeably the swelling ratio in water.

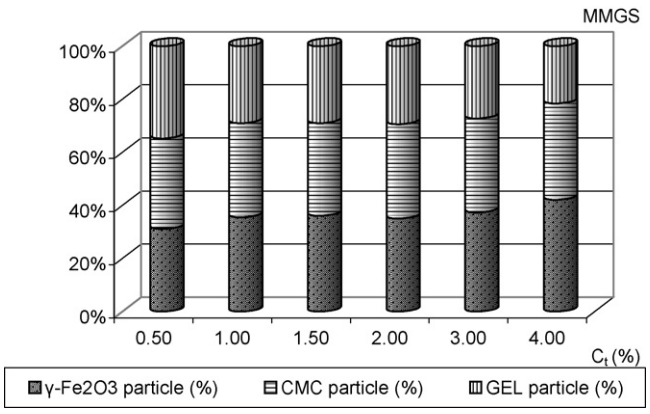

Fig. 10. Influence of the surfactant mixture concentration (Span 80 and Tween 80) on the MMGS series particles composition (CMCNa:GEL:γ-Fe_2O_3 = 38.4:25.6:36; r_{PA} = 71.43).

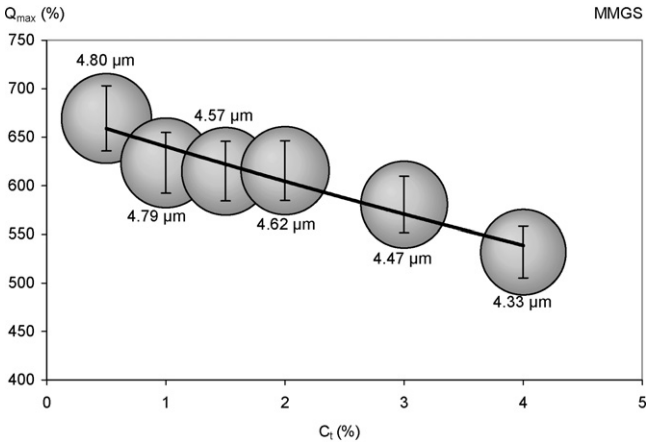

Fig. 11. Influence of the surfactant mixture concentration (Span 80 and Tween 80) on the MMGS series particles size and swelling degree (CMCNa:GEL:γ-Fe_2O_3 = 38.4:25.6:36; r_{PA} = 71.43).

3.3. Biological and biomedical properties of the particles

Having obtained the aforementioned particles with the eventual aim of using them for transport and controlled release of target-drugs, we studied their biological properties.

3.3.1. Evaluation of toxicity

To synthetise magnetic micro-/nanoparticles, excepted CMCNa and GEL which are biocompatible and non-toxic polymers, toxic chemicals were used such as the crosslinking agent, the solvent (toluene) and the surfactants. Use of these particles in contact or inside the human organism requires the evaluation of their toxicity degree. The lethal dose (LD_{50}) was determined and data are given in Table 2.

LD_{50} values show no or low toxicity of obtained particles with the different types of surfactant even if values obtained with Span and Tween (MMGS2 sample) are much more smaller than other ones.

Table 2
LD_{50} values for microparticles obtained with different surfactants.

Sample	GEL	CMCNa	MMGB5	MMGS2
LD_{50} (mg/kg body)	8190	7700	8820	1070

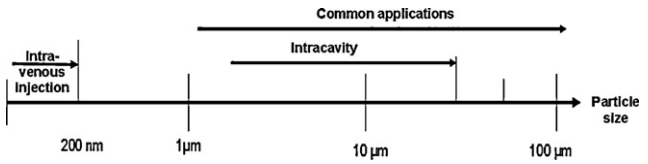

Scheme 2. Administration of particles as a function of their size.

3.3.2. Inclusion and release of drugs

The applications and the administration mode of drug loaded magnetic particles depend on their size (Scheme 2).

MMGB5 and MMGB17 series were chosen for such experiments. Drugs were Cefotaxime (an antibiotic) and Methotrexate (an anti-tumoral drug).

Inclusion was carried out by diffusion of drug from an aqueous solution within particles beforehand swollen at equilibrium. The kinetics of the inclusion process is shown in Fig. 12a.

Drug inclusion developed quickly and equilibrium was reached after 90–120 min. Curves are typical of a diffusion-controlled process. The maximal quantity of drug included is in good agreement with the swelling ratio of the particles. It may focus on the higher quantity of included MTX compared with CFTS (about 25%) due to the di-anion character of the latter, leading to a higher solubility.

The release of the two drugs was performed more quickly than inclusion. A stable period was reached after around 60 min. (Fig. 12b) and CFTS was released more quickly than MTX due to weaker interactions with polymers of the particle network.

The maximal quantity of drug (at equilibrium) which is included in or released from particles depends on the swelling capacity in aqueous media, the latter being dependent on different parameters such as the crosslinking density, the composition of particles and their size. Fig. 13 compares the quantity of included CFTS and then released as a function of the maximal swelling ratio in water for MMGB series 4 particles. There is a direct correlation between these two characteristics and the drug release is almost total. Similar results were obtained whatever the series of particles.

To obtain more information on the drug transport mechanism by the hydrogel forming the particle matrix, the Korsemeyer–Peppas relation (5) was applied (Delgado et al., 2002):

$$\frac{M_t}{M_\infty} = k \cdot t^n \quad (5)$$

M_t and M_∞ being the total quantities of included (released) drug at time t, respectively at the end of the inclusion (release) process, t, the time, k the rate constant and n the process order. The values obtained for the two kinetic parameters and the CFTS-loaded particles are given in Table 3.

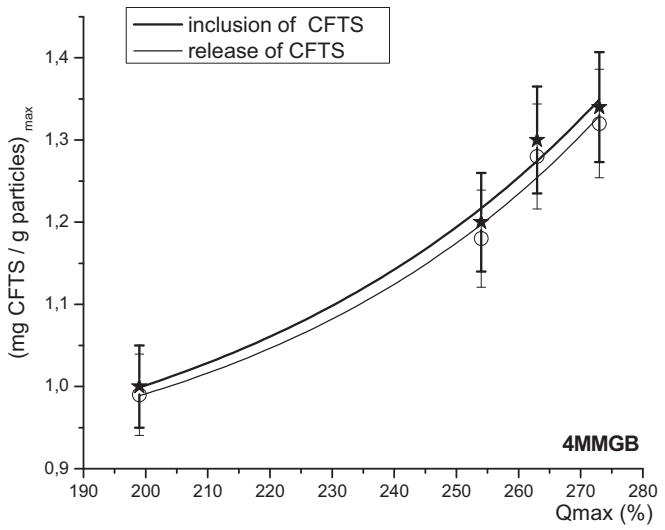

Fig. 13. Influence of swelling degree on the CFTS inclusion and release capacities for MMGB series 4 particles (CMCNa:GEL:γ-Fe_2O_3 = 38.4:25.6:36; r_{PA} = 71.43; surfactants Brij 52 and Tween 80).

Table 3
Values of k and n coefficients from Korsemeyer–Peppas relation.

Series	Inclusion		Release	
	k (min^{-1})	n	k (min^{-1})	n
MMGB17	0.053	0.68	0.106	0.60
MMGB5	0.093	0.55	0.165	0.46

k Values demonstrate that release process has a larger rate than inclusion. Moreover, from n values, the two processes are close from Fick model for particles from MMGB5. Similar results are obtained with MTX.

3.3.3. Antibacterial activity of drug loaded particles

In preparation for potential biomedical applications resulting from the absence of toxicity of particles and their capacity to include and release CFTS, the antibacterial activity has to be demonstrated.

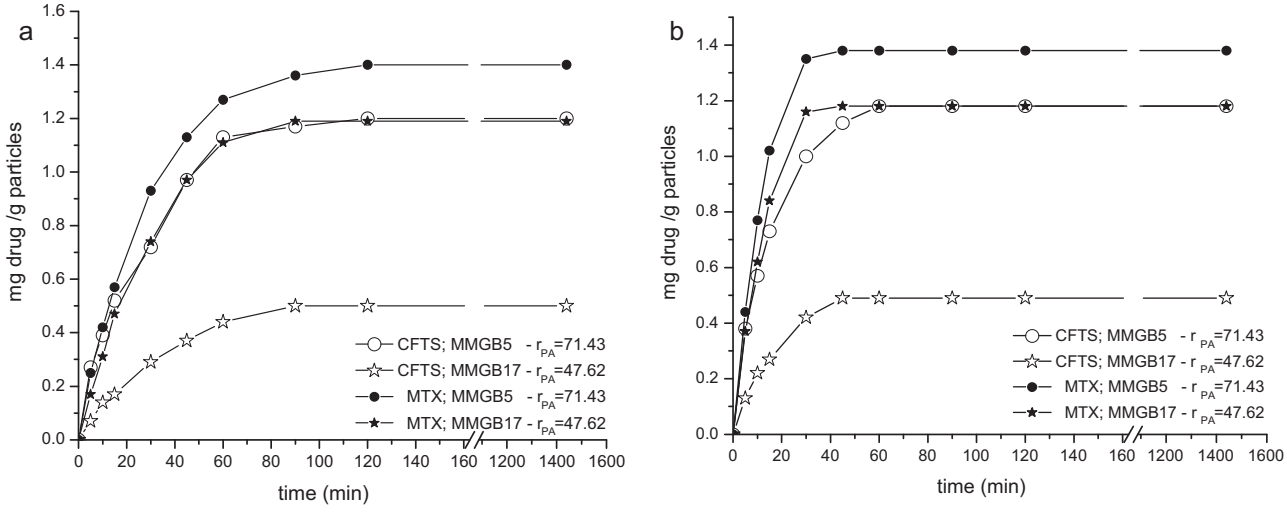

Fig. 12. Kinetics of inclusion (a) and release (b) of CFTS and MTX within MMGB17 and MMMG5 particles (CMCNa:GEL:γ-Fe_2O_3 = 38.4:25.6:36; C_t = 0.225%; r_{PA} = 71.43).

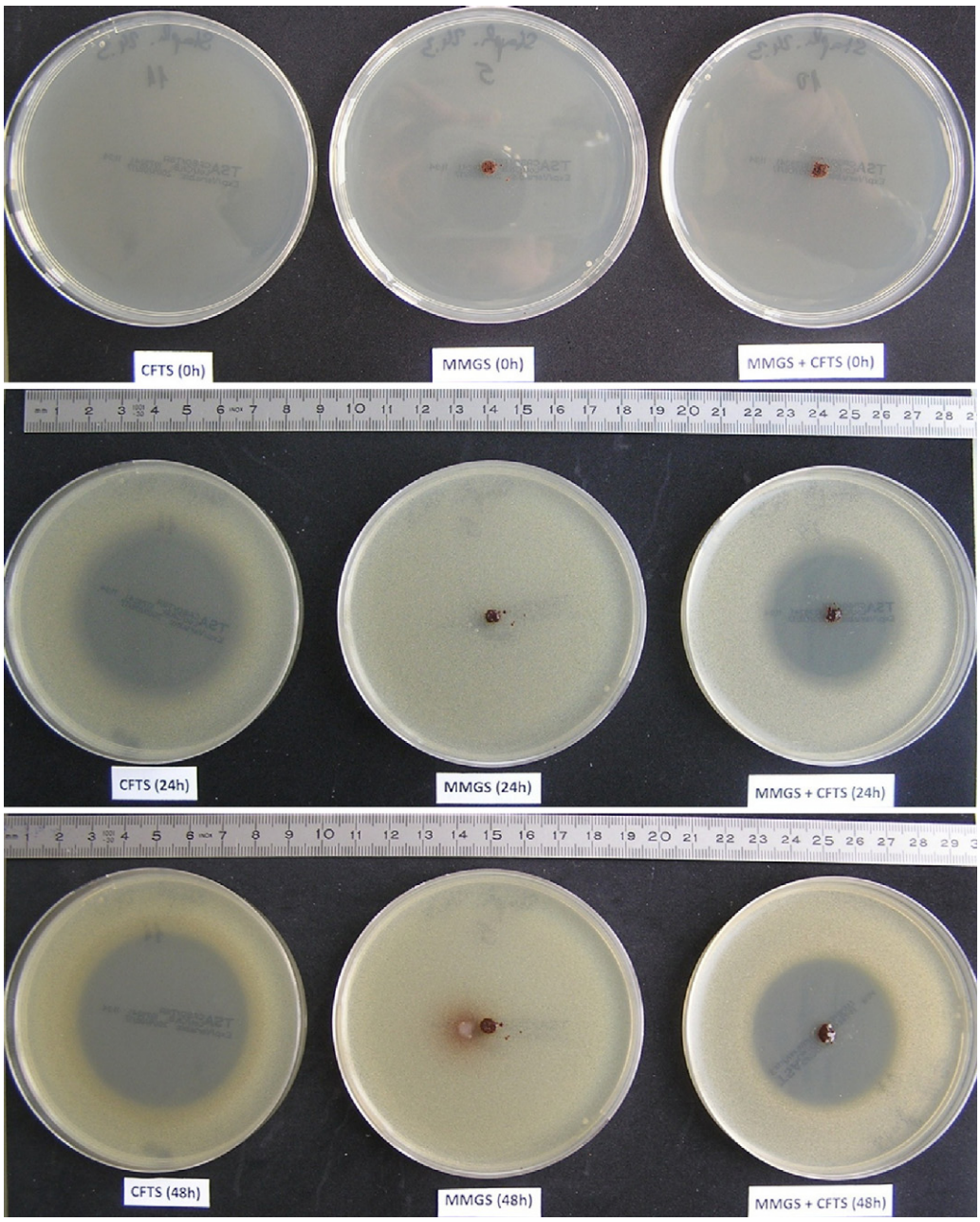

Fig. 14. Antibacterial activity tests of MMGS particles loaded with CFTS on *Staphylococcus aureus* ATCC 25923.

MMGB5 and MMGS2 were tested on two bacterial strains: Gram-negative germs (*Pseudomonas aeruginosa* ATCC 27853) and gram-positive ones (*Staphylococcus aureus* ATCC 25923). The inhibition zone around the tested particles was measured after 24 and 48 h. All the tested systems have proven a bactericide activity *vis-à-vis* the two bacterial strains. This was shown for MMGS particles loaded with CFTS tested on *S. aureus* ATCC 25923. These particles demonstrate a bactericide activity even after long times (48 h) when the non-loaded particles do not exhibit such an activity (Fig. 14).

4. Conclusions

Interpenetrated network type magnetic micro- and nanoparticles based on natural polymers (carboxymethylcellulose and gelatin) were elaborated using an inverse emulsion crosslinking process. The composition, the morphology, swelling in water characteristics, the capacity to include and release water soluble drugs of these particles depend on elaboration process parameters such as the polymer ratio, the polymer mixture/crosslinking agent (respectively maghemite) ratio, or the nature and the concentration of the surfactant. The ability to include drugs is directly correlated with the swelling degree and the gelatin content within the particles. Polymer–drug systems elaborated under particles retain their bactericide activity for at least 48 h. The absence of toxicity, associated with the bactericide activity, make these systems potential drug carriers.

Acknowledgement

Roger Hiorns was acknowledged for his help in editing the article.

References

Alexiou, C., Arnold, W., Hulin, P., Klein, R.J., Renz, H., Parak, F.G., Bergmann, C., Lübbe, A.S., 2001. Magnetic mitoxantrone nanoparticle detection by histology, X-ray and MRI after magnetic tumor targeting. J. Magn. Magn. Mater. 225, 187–193.

Arias, J.J., Gallardo, V., Gómez-Lopera, S.A., Delgado, A.V., 2005. Loading of 5-fluorouracil to poly(ethyl-2-cyanoacrylate) nanoparticles with a magnetic core. J. Biomed. Nanotechnol. 1–2, 214–223.

Bellusci, M., La Barbera, A., Seralessandri, L., Padella, F., Piozzi, A., Varsano, F., 2009. Preparation of albumin–ferrite superparamagnetic nanoparticles using reverse micelles. Polym. Int. 58, 1142–1147.

Bergemann, C., Müller-Schulte, D., Oster, J., A Brassard, L., Lübbe, A.S., 1999. Magnetic ion-exchange nano- and microparticles for medical, biochemical and molecular biological applications. J. Magn. Magn. Mater. 194, 45–52.

Bradstreet, R.B., 1965. The Kjedahl Method for Organic Nitrogen. Academic Press, New York, pp. 1–66.

Chen, J., Yang, L., Liu, Y., Ding, G., Pei, Y., Li, J., Hua, G., Huang, J., 2005. Preparation and characterization of magnetic targeted drug controlled-release hydrogel microspheres. Macromol. Symp. 225, 71–80.

Czajkowska, T., Graczyk, J., Kryziak, B., Stetkiewicz, J., 1978. Acute toxic effects of trimethyl and triethyl phosphates. J. Med. Pharm. 29, 393–398.

Delgado, M., Spanka, C., Kerwin, L.D., Wentworth Jr., P., Janka, K.D., 2002. A tunable hydrogel for encapsulation and controlled release of bioactive proteins. Biomacromolecules 3, 262–271.

Finney, D.J., 1978. Statistical Method in Biological Assay. Charles Griffin & Co, London, pp. 394–401.

Goya, G.F., Grazú, V., Ibarra, M.R., 2008. Magnetic nanoparticles for cancer therapy. Curr. Nanosci. 4, 1–16.

Hassan, E.E., Parish, R.C., Gallo, J.M., 1992. Optimized formulation of magnetic chitosan microspheres containing the anticancer agent, oxantrazole. Pharm. Res. 9, 390–397.

Honga, R., Li, J., Wang, J., Li, H., 2007. Comparison of schemes for preparing magnetic Fe_3O_4 nanoparticles. China Particuol. 5, 186–191.

Kohler, N., Sun, C., Fichtenholtz, A., Gunn, J., Fang, C., Zhang, M., 2006. Methotrexate-immobilized poly(ethylene glycol) magnetic nanoparticles for MR Imaging and drug delivery. Small 2, 785–792.

Laurent, S., Forge, D., Port, M., Roch, A., Robic, C., Elst, L.V., Muller, R.N., 2008. Magnetic iron oxide nanoparticles: synthesis, stabilization, vectorization, physicochemical characterizations, and biological applications. Chem. Rev. 108, 2064–2110.

Levy, M., Wilhelm, C., Siaugue, J.M., Horner, O., Bacri, J.C., Gazeau, F., 2008. Magnetically induced hyperthermia: size-dependent heating power of γ-Fe_2O_3 nanoparticles. J. Phys.: Condens. Matter 20, 204133–204138.

Longo, W.E., Iwata, H., Lindheimer, T., Goldberg, E.P., 1982. Preparation of hydrophilic albumin microspheres using polymeric dispersing agents. J. Pharm. Sci. 72, 1323–1328.

Lu, M., Bai, S., Yang, K., Sun, Y., 2007. Synthesis and characterization of magnetic polymer microspheres with a core–shell structure. China Particuol. 5, 180–185.

Lübbe, A.S., Bergemann, C., Huhnt, W., Fricke, T., Riess, H., Brock, J.W., Huhn, D., 1996a. Preclinical experiences with magnetic drug targeting: tolerance and efficacy. Cancer Res. 56, 4694–4701.

Lübbe, A.S., Bergemann, C., Riess, H., Schriever, F., Reichardt, P., Possinger, K., Matthias, M., Huhn, D., 1996b. Clinical experiences with magnetic drug targeting: a phase I study with 4′-epidoxorubicin in 14 patients with advanced solid tumors. Cancer Res. 56, 4686–4693.

Ma, Z., Liu, H., 2007. Synthesis and surface modification of magnetic particles for application in biotechnology and biomedicine. China Particuol. 5, 1–10.

McBain, S.C., Yiu, H.P., Dobson, J., 2008. Magnetic nanoparticles for gene and drug delivery. Int. J. Nanomed. 3, 169–180.

Massart, R., 1980. Préparation de ferrofluides aqueux en l'absence de surfactant; comportement en fonction du pH et de la nature des ions présents en solution. C. R. Acad. Sci. Ser. C, Paris 1, 291.

Nagano, H., Machida, Y., Iwata, M., Imada, T., Noguchi, Y., Matsumoto, A., Nagai, T., 1997. Preparation of magnetic granules containing bleomycin and its evaluation using model esophageal cancer. Int. J. Pharm. 147, 119–125.

Nenitescu, C.D., 1980. In: Didactica si Pedagogica, Chimie organica, vol. 1. Bucarest.

Pankhurst, A.Q., Connolly, J., Jones, S.K., Dobson, J., 2003. Applications of magnetic nanoparticles in biomedicine. J. Phys. D: Appl. Phys. 36, 167–181.

Ramanujan, R.V., Chong, W.T., 2004. The synthesis and characterization of polymer coated iron oxide microspheres. J. Mater. Sci.: Mater. Med. 15, 901–908.

Ruiz-Hernandez, E., Lopez-Noriega, A., Arcos, D., Vallet-Regı, M., 2008. Mesoporous magnetic microspheres for drug targeting. Solid State Sci. 10, 421–426.

Tataru, G., 2009. Polymeric systems under particular form for immobilization and controlled release of biologically active matter. PhD Thesis, "Gh.Asachi" Technical University of Iasi, Romania and Universite de Pau et des Pays de l'Adour, France.

Verdinelli, V., Messina, P.V., Schulz, P.C., Vuano, B., 2008. Hydrophile–lipophile balance (HLB) of *n*-alkane phosphonic acids and their salts. Colloids Surf. A: Physicochem. Eng. Aspects 316, 131–135.

Widder, K., Flouret, G., Senyei, A.E., 1979. Magnetic microspheres: synthesis of a novel parenteral drug carrier. J. Pharm. Sci. 68, 79–82.

Yang, J., Park, S.B., Yoon, H.G., Huh, Y.M., Haam, S., 2006. Preparation of poly ε-caprolactone nanoparticles containing magnetite for magnetic drug carrier. Int. J. Pharm. 324, 185–190.